NUCLEAR SCIENCE AND TECHNIQUES **26**, 020101 (2015)

Introduction of the X-ray diffraction beamline of SSRF*

YANG Tie-Ying (杨铁莹),[1] WEN Wen (文闻),[1] YIN Guang-Zhi (阴广志),[1] LI Xiao-Long (李晓龙),[1] GAO Mei (高梅),[1] GU Yue-Liang (顾月良),[1] LI Li (李丽),[1] LIU Yi (柳义),[1] LIN He (林鹤),[1] ZHANG Xing-Min (张兴民),[1] ZHAO Bin (赵滨),[1] LIU Ting-Kun (刘亭坤),[1] YANG Ying-Guo (杨迎国),[1] LI Zhong (黎忠),[1] ZHOU Xing-Tai (周兴泰),[1] and GAO Xing-Yu (高兴宇)[1,†]

[1] *Shanghai Institute of Applied Physics, Chinese Academy of Sciences, Shanghai 201204, China*

(Received September 29, 2014; accepted in revised form November 7, 2014; published online April 20, 2015)

The X-ray diffraction beamline developed at Shanghai Synchrotron Radiation Facility (SSRF)is located at the BL14B1 bending magnet port of the 3.5 GeV storage ring. The beamline optics is based on a collimating mirror, a sagittally focused double crystal monochromator and a focusing mirror. Photon flux of 4.43×10^{11} phs/s at 10 keV is obtained. The primary instrument equipped in the experimental end-station is a Huber 5021 six-cycle diffractometer. BL14B1 is a general purpose X-ray diffraction beamline and focused on material science, condensed matter physics and other relevant fields looking for structural information.

Keywords: Synchrotron radiation, X-ray diffraction, BL14B1, SSRF

DOI: 10.13538/j.1001-8042/nst.26.020101

I. INTRODUCTION

X-ray diffraction technique is widely used to obtain structure of crystalline materials under various conditions of temperature, pressure, electric and magnetic field, etc. [1]. As a phase-I beamline at Shanghai Synchrotron Radiation Facility (SSRF), BL14B1 is dedicated to X-ray diffraction studies on materials science, condensed matter physics and other relevant fields. Polycrystalline powder, surface and interface of film/ultra-thin films, and microstructure of nano-materials have been the main research objectives.

Since its commissioning to users in 2009, BL14B1 has allocated user beamtime of over 20 000 h. Over 500 user proposals have been executed. The beamline and the experimental end-station were upgraded for several times to facilitate the user experimentss and to become more convenient to operate. In this paper, the beamline optics, the experimental end-station, the experimental methods, and its commissioning results are reported.

II. SOURCE AND BEAMLINE OPTICS

SSRF is composed of a 3.5 GeV electron storage ring, 3.5 GeV booster and a 150 MeV linac. The beam current in the storage ring is 240 mA. Parameters of the bending magnet, as source of beamline BL14B1, are given in Table 1, and layout of the beamline is shown in Fig. 1.

The BL14B1 beamline has three critical components: a collimating mirror, a sagittally focused double crystal monochromator, and a focusing mirror, which are 21, 24 and 30 m away from the source, respectively. The collimating mirror is used to collimate the beam in vertical direction into parallel light, improving the energy resolution. The monochromator consists of a flat water-cooled first crystal and a dynamically bent sagittal crystal to focus the beam in horizontal direction to the sample point. The focusing mirror further focalize the beam in vertical direction to the sample point.

Angular acceptance of the beamline, determined mainly by the water-cooling quad-blade slit (Slit1) in front of the collimating mirror, is 2.5 mrad and 0.12 mrad in horizontal and vertical directions, respectively. Energy range of the beamline is mainly determined by the grazing incidence angle of the collimating mirror. The collimating mirror and focusing mirror are half Rh-coated Si-based cylindrically bend mirror. Grazing incidence angle of 2.8 mrad is used, hence a cutting-off energy of about 22 keV. Reflection of the collimating and focusing mirrors can further suppress higher order harmonics significantly.

Three beryllium windows are placed after the collimating mirror, monochromator and focusing mirror, respectively, to maintain different vacuum levels. A beam block is installed behind the monochromator to block the white light and bremsstrahlung radiation reflected by collimating mirror. Two monochromatic slits are positioned at the back of the focusing mirror (Slit2) and the end of beamline (Slit3) to stop the stray light and improve angular resolution. The first crystal of monochromator absorbs almost all the radiation after collimating mirror. Power density of the crystal reaches 0.4 W/mm^2, hence the need of water cooling.

Performance of the beamline is evaluated by measuring absorption and diffraction patterns from standard inorganic powder samples. The energy range is examined at 100 mA and 200 mA using the *K*-edge absorption spectrum of CaO (4.0385 keV) and $RuCl_3$ (22.117 keV). The energy resolution at 8.9 keV was estimated at 2.47×10^{-4} by width of the *K*-edge absorption spectrum of Cu at 100 mA and 200 mA. This is a popular and easy method. However, the precision and range are limited by the natural width. So, 10 keV XRD pattern of NIST SRM660a LaB_6 standard powder was used to examine the energy resolution. The instrumental resolution function can be figured out from the diffraction peaks. The

* Supported by the National Natural Science Foundation of China (Nos. 11405253, U1332205, 21203235 and 11175239)

† Corresponding author, gaoxingyu@sinap.ac.cn

TABLE 1. Parameters of the bending magnet source for the BL14B1 beamline

Beam energy (GeV)	Natural emittance (nm rad)	(Coupling)	Beam current (mA)	Bending field (T)	Beam size and emittance			
					σ_x(μm)	σ_y(μm)	σ'_x(μrad)	σ'_y(μrad)
3.5	3.9	1.0%	240	1.27	70	22	114	1.97

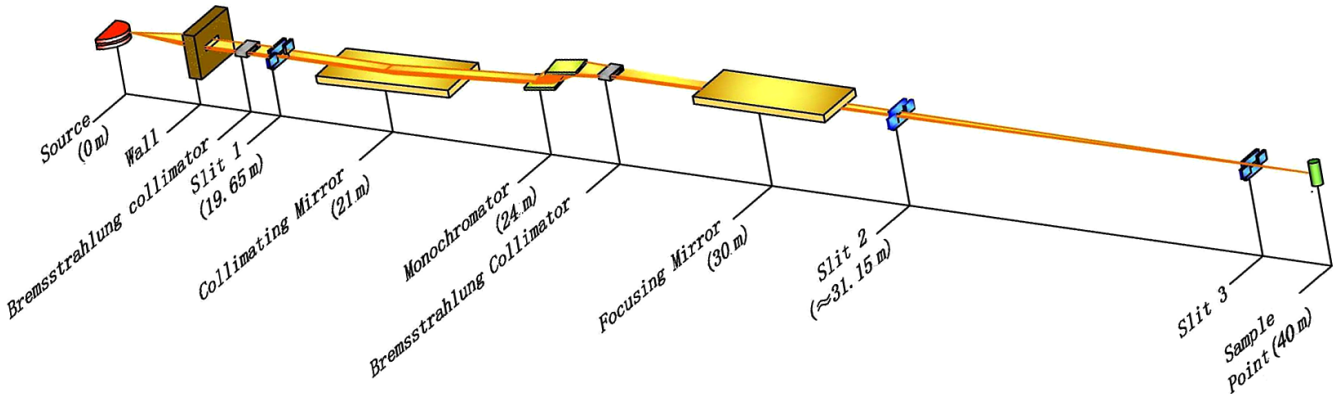

Fig. 1. (Color online) Layout of the BL14B1 beamline.

measurement result is 1.91×10^{-4} at 200 mA. Spot size and angular divergence at focus point is measured with a quad-blade slit and an ionization chamber at 100 mA and 200 mA. Spot size is defined as FWHM (Full width at half maximum) of intensity distribution profile, which can be obtained by scanning the slit horizontally and vertically. Using the measurement results of spot size at two positions of the beamline, the angular divergence can be calculated. The spot size is $0.21\,\text{mm}(H) \times 0.13\,\text{mm}(V)$, while the angular divergence is $1.284 \times 0.090\,\text{mrad}^2$ at 200 mA for the focus mode. Photon flux was measured using an ionization chamber, according to the formula $I = Ee\eta N/\varepsilon$, where I is the intensity of current, E is the X-ray energy, N is the number of photons, e is the electron charge, and η is the absorption efficiency. Photon flux of 4.43×10^{11} phs/s at 10 keV was obtained. Table 2 lists the main specifications of the beamline.

III. EXPERIMENTAL END-STATION CONFIGURATION

As shown in Fig. 2, a Huber 5021 six-cycle diffractometer is equipped in the experimental end-station to enable multi-dimensional orientations of samples. Ceramic, crystal, metallic, polymeric and other samples can be effectively measured.

For data collection, a Bede point detector and image plate detector are used to allow the measurements in high-resolution mode or fast mode. In 2012, the Mar345 image plate detector was replaced by an Mar225 CCD and related accessories, such as shutter, software, etc. The new detector is of sub-second time resolution and much faster readout time. A Si microstrip detector (Mythen 1K) is also equipped, together with the data control software and acquisition method. The photon flux is monitored using an on-line ionization chamber. In addition, a Si(111) crystal analyzer improves the angle resolution greatly.

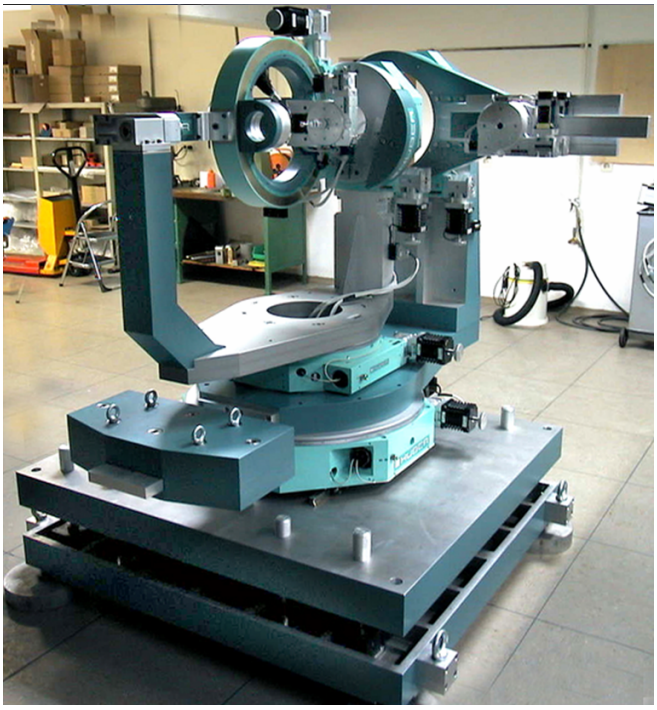

Fig. 2. (Color online) Huber 5021 6-cycle diffractometer.

A prominent advantage of the synchrotron-based techniques is the very high photon flux, which is necessary for *in situ* studies, unlike conventional XRD facilities. The *in situ* experiments can provide real time studies of the sample at non-ambient condition, which otherwise might change. The *in situ* experiments in MRI TC-radiation or Linkam high temperature chambers (Fig. 3) provide real time studies of samples in non-ambient condition.

TABLE 2. Parameters of the bending magnet source for the BL14B1 beamline

Parameters		Design specifications	Measurement results
Energy range(keV)		4–22	4–22
Energy resolution ($\Delta E/E$)		$\leq 2 \times 10^{-4}$	1.91×10^{-4}
	Photon Flux (phs/s@10 keV@300 mA)	$\geq 2 \times 10^{11}$	4.43×10^{11}
Focus Mode	Spot Size ($H \times V$, mm^2)	$\leq 0.4 \times 0.4$	0.21×0.13
	Divergence ($H \times V$, mrad^2)	$\leq 2.5 \times 0.2$	1.284×0.090
	Photon Flux (phs/s@10 keV@300 mA)	$\geq 2 \times 10^{11}$	4.43×10^{11}
Non-focus Mode	Spot Size ($H \times V$, mm^2)	$\leq 0.4 \times 3.0$	0.21×1.14
	Divergence ($H \times V$, mrad^2)	$\leq 2.5 \times 0.02$	1.276×0.013

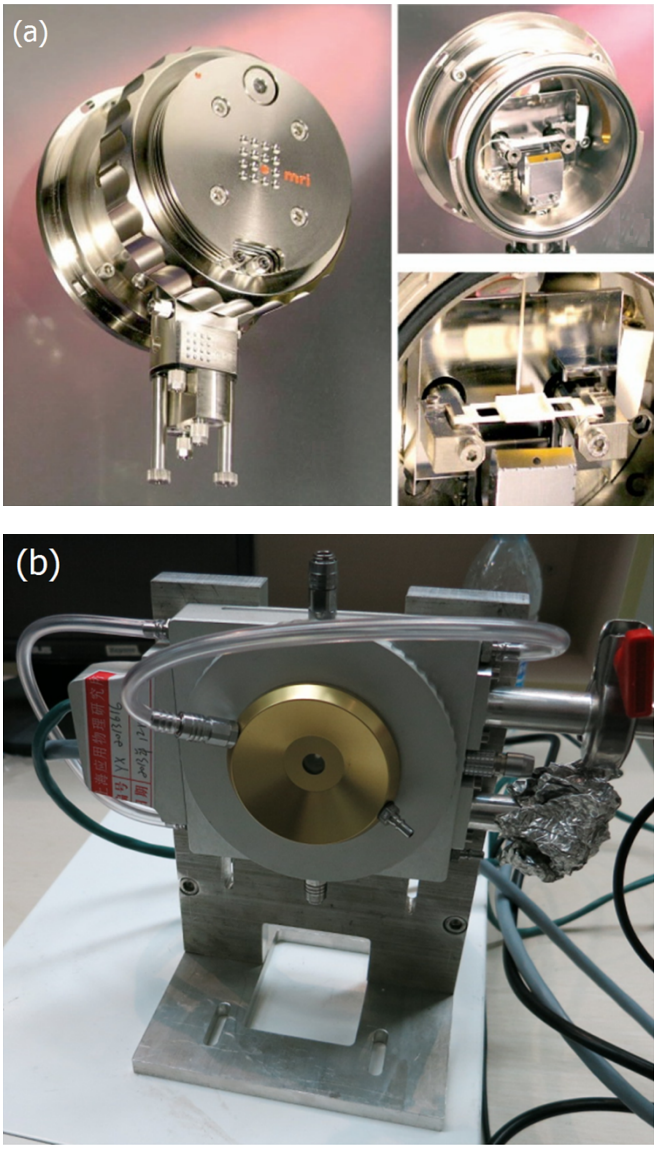

Fig. 3. (Color online) The MRI TC-radiation (a) and Linkam (b) high-T chambers.

The MRI TC-radiation high temperature chamber (Fig. 3(a)) is mainly used in inert gas environment or in vacuum. A sample can be heated to 800 °C under inert gas protection by a direct Mo strip heater. Using a radiation heater under vacuum condition, the temperature can reach 1100 °C,thus being suitable for measuring powder and metallic samples. The samples are loaded into an Al_2O_3 crucible. The diffraction experiments are carried out in reflection mode. Typical size of a metallic sample is 10 mm × 10 mm × 1.5 mm. A *K*-type thermocouple is soldered to the sample surface to measure the temperature. The MRI chamber can be evacuated to about 10^{-2} Pa. Fig. 3(b) shows the Linkam high-T chamber. Is can achieve up to 1500 °C in vacuum and is suitable for XRD experiment in transmission mode, for materials samples of alloy, polymeric film, etc.

In situ electric field device and *in situ* high/low-temperature chamber for thin films are available to users. Besides, the beamline has a supporting laboratory equipped with fume hood, glove box, vacuum oven, balance, etc., for sample preparation by the users.

IV. EXPERIMENTS METHODS AND EXAMPLES

The experimental techniques available include high-resolution powder diffraction (HRXRD), X-ray reflectivity (XRR), grazing incidence X-ray diffraction (GIXRD), reciprocal space mappings (RSMs), atomic pair distribution function analysis (PDF), and total reflection X-ray fluorescence spectroscopy (TXRF).

A. High-resolution powder diffraction

This method can be used for measuring samples of heterogeneous catalysts, compounds for hydrogen storage, electrode materials for lithium battery applications, ferroelectric compounds, thermo-electric compounds, super- conductor materials, etc. Because of the monochromatic high flux and highly collimated beams, the main advantages of synchrotron-based powder XRD against conventional XRD include no $K\alpha_2$ diffraction peaks, higher signal/noise ratio and much better angular resolution.

Professor Chen's group used experimental data collected at BL14B1 to determine the crystal structure by powder XRD pattern indexing, crystal lattice determination, space group analysis and lattice constant calculation, overlapped diffraction peaks de-convolution, determining the intensity of

each diffraction peak and calculating related structure amplitude, etc [2]. The significance of their work is synthesis and characterization of a new hydrogen storage material, light metal ammonia borane, expands the research field of B-N related chemicals, and provides theoretical basis and technical support for new hydrogen storage materials.

B. X-ray reflectivity

XRR technique uses low angle (generally $2\theta < 10°$) $\theta \sim 2\theta$ scan mode, known also as small angle diffraction. The interface reflection occurs due to different X-ray refractive index of the medium layers. XRR signal results from periodic diffraction of multilayer. Multilayer iterative calculation method of XRR was first given by L. G. Parratt [3]. The matrix calculation method of XRR for non-ideal interface was deduced later [4, 5]. XRR is widely applied to samples of film/ultra-thin film and multilayer, and the electron density, thickness, roughness of films, superlattices, etc. can be obtained. Thickness and optical constants of solgel derived polyvinylpyrrolidone/ZrO_2 films were determined by Professor Xu Yao's group using XRR [6].

C. Grazing incidence X-ray diffraction

GIXRD is widely used to study super-conductivity, ferroelectric thin film, thermo-electric thin film, semiconducting thin film, wet-epitaxially-grown organic film, polymer thin film transistors, etc. Thin-films as thin as one atomic layer can be grown on single crystal substrates, and analyzed by GIXRD. With a very small incidence angle, one can expect to have much higher cross-section for detection, thus to increase the sample signal and greatly suppress the signal from substrate.

While using the point detector, one can collect data either in-plane or out-plane. Fixing the incidence angle (eg, $\theta = 0.2°$), one can scan the 2θ arm horizontally and collect the in plane diffraction signal from the sample. This signal is the essential diffraction signal from the sample, which displays long range ordering perpendicular to the sample surface. One can collect the out-of-plane signal by scanning the 2θ arm vertically. The sample signal, which displays long-range ordering parallel to the normal of the sample surface, can be studied. Using the 2D image plate detector, the in-plane and out-plane modes can be further studied, after the incidence angle of the film is determined using the point detector.

Professor Pei Jian's group studied the structure of two thin organic films of IIDDT and IIDT [7]. They found four strong diffraction peaks of IIDDT, using GIXRD technique, but just a weak diffraction peak for IIDT. These indicate that IIDDT has a regular long range ordering along the (001) direction, whereas IIDT is more likely with an amorphous phase. Further, the mobility and on/off ratio of the IIDDT, which are critical factors for field-effect transistors, were superior to those of IIDT, thus revealing a clear correlation between the structure and property. The structures of the IIDDT and IIDT films were confirmed using AFM technique.

D. Reciprocal space mappings

Reciprocal space mappings is used to study the domain structure, strain relax, orientation difference and lattice mismatching of crystal or film sample. Professor Yang Ping from Singapore Light Source successfully measured $BiFeO_3$ thin films grown on different substrates at BL14B1, using reciprocal space mapping techniques [8]. For sample of $BiFeO_3$/$LaAlO_3$, the diffraction peak of (103) was a triplet, indicating a monoclinic Mc phase instead of the M_A or M_B phase reported in previous studies.

E. Atomic pair distribution function analysis

Atomic pair distribution function (PDF) method attracts much interest recent years [9, 10]. By illustrating the atomic pair correlation information, PDF is useful in condensed matter physics and catalyst chemistry, especially for nanoscale systems. PDF gives the atomic correlation information up to several nanometers, hence a complement to EXAFS (Extended X-ray absorption fine structure) where the correlation length usually is limited to the (next) nearest neighbors (a few angstroms).

The PDF measurement in BL14B1 involves usage of diffractometer for large 2θ angle and higher X-ray energy. We have managed to use 18 keV X-ray and a wide 2θ scanning angle ($> 150°$, corresponds to a Q range of ~ 17 Å^{-1}) for PDF studies. The setup can be used for amorphous (glass or liquid) and nano-material studies.

F. Total reflection X-ray fluorescence spectroscopy

Total reflection X-ray fluorescence (TXRF) spectroscopy is developed in collaboration with the users. As a complementary method, TXRF analysis, a non-destructive elemental analysis technique, is widely used to determine the depth profiles of trace elements in semiconductor, thin layers on substrate and adsorbed molecules [11–14]. Combined TXRF with XRR, one is able to conduct non-destructive depth profiling of layered samples. Professor Li Wenbin's group analyzed the structure of Si(substrate)/W/Ni/Ti/N multi-layer using both reflectivity and grazing incidence fluorescence measurements. Combination of the two data sets (refined) gave more precise structural parameters [15].

V. SUMMARY AND OUTLOOK

BL14B1 is a high-resolution X-ray diffraction beamline. The beamline optics and end-station configuration are well suitable for polycrystalline powder and surface/interface of films. Diffraction techniques of GIXRD and RSM, *in situ*

experimental devices especially, have been realized on the beamline. These greatly promote research programs of the beamline users, which has been growing rapidly. However, according to publication analysis across the world, beamlines dedicated to powder diffraction studies did much better in productivity, such as the powder diffraction beamline in Australian Synchrotron, Diamond I11, and Spring-8 BL02B2. As a general purpose diffraction beamline, BL14B1 at SSRF needs to further strengthen its research on powder diffraction. It surely requires efforts in the update of the beamline towards this direction. Especially, phase II beamline construction engineering project will include one surface diffraction beamline and one Laue microdiffraction beamline. It is reasonable for BL14B1 to focus on powder diffraction.

[1] Warren B E. X–ray diffraction. Massachusetts: Addison-Wesley Publishing Company, Inc. Reading, 1969.

[2] Wu C Z, Wu G T, Xiong Z T, *et al*. $LiNH_2BH_3$-NH_3BH_3: structure and hydrogen storage properties. Chem Mater, 2010, **22**: 3–5. DOI: 10.1021/cm903167b

[3] Parratt L G. Surface studies of solids by total reflection of X-Rays. Phys Rev, 1954, **95**: 359–369. DOI: 10.1103/PhysRev.95.359

[4] Névot L and Croce P. Caractérisation des surfaces par réflexion rasante de rayons X. Application à l'étude du polissage de quelques verres silicates. Rev Phys Appl, 1980, **15**: 761–779. DOI: 10.1051/rphysap:01980001503076100

[5] Vidal B and Vincent P. Metallic multilayers for X-rays using classical thin-film theory. Appl Opt, 1984, **23**: 1794–1801. DOI: 10.1364/AO.23.001794

[6] Jia H B, Sun J H, Xu Y, *et al*. Determination of thickness and optical constants of solgel derived olyvinylpyrrolidone/ZrO_2 films from transmission spectra using different dispersion models. Appl Opt, 2012, **51**: 6937–6944. DOI: 10.1364/AO.51.006937

[7] Lei T, Cao Y, Fan Y L, *et al*. High-performance air-stable organic field-effect transistors: isoindigo-based conjugated polymers. J Am Chem Soc, 2011, **133**: 6099–101. DOI: 10.1021/ja111066r

[8] Chen Z H, Luo Z L, Huang C W, *et al*. Low-symmetry monoclinic phases and polarization rotation path mediated by epitaxial strain in multiferroic $BiFeO_3$ thin films. Adv Funct Mater, 2011, **21**: 133–138. DOI: 10.1002/adfm.201001867

[9] Billinge S J L and Kanatzidis M G. Beyond crystallography: the study of disorder, nanocrystallinity and crystallographically challenged materials with pair distribution functions. Chem Commun, 2004, **21**: 749–760. DOI: 10.1039/b309577k

[10] Billinge S J L and Levin I. The problem with determining atomic structure at the nanoscale. Science, 2007, **316**: 561–565. DOI: 10.1126/science.1135080

[11] Becker R S, Golovchenko J A and Patel J R. X-ray evanescent-wave absorption and emission. Phys Rev Lett, 1983, **50**: 153–156. DOI: 10.1103/PhysRevLett.50.153

[12] Kregsamer P, Streli Christina, Wobrauschek P, *et al*. Synchrotron radiation-excited glancing incidence XRF for depth profile and thin-film analysis of light elements. X–ray Spectrom, 1999, **28**: 292–296. DOI: 10.1002/(SICI)1097-4539(199907/08)28:43.3.CO;2-1

[13] Klockenkämper R. Challenges of total reflection X-ray fluorescence for surface- and thin-layer analysis. Spectrochim Acta Part B, 2006, **61**: 1082–1090. DOI: 10.1016/j.sab.2006.09.007

[14] Li W, Zhu J, Li H, *et al*. Ni layer thickness dependence of the interface structures for Ti/Ni/Ti trilayer studied by X-ray standing waves. ACS Appl Mater Interfaces, 2013, **5**: 404–409. DOI: 10.1021/am3024614

[15] Yang X Y, Li W B, Zhu J T, *et al*. Structural characterization of multilayer using the analysis combining GIXRF with GIXRR method. Proc SPIE 9068, Eighth International Conference on Thin Film Physics and Applications, 90680X, December 16, 2013. DOI: 10.1117/12.2053960